

## Supplementary note

### Digital Holography

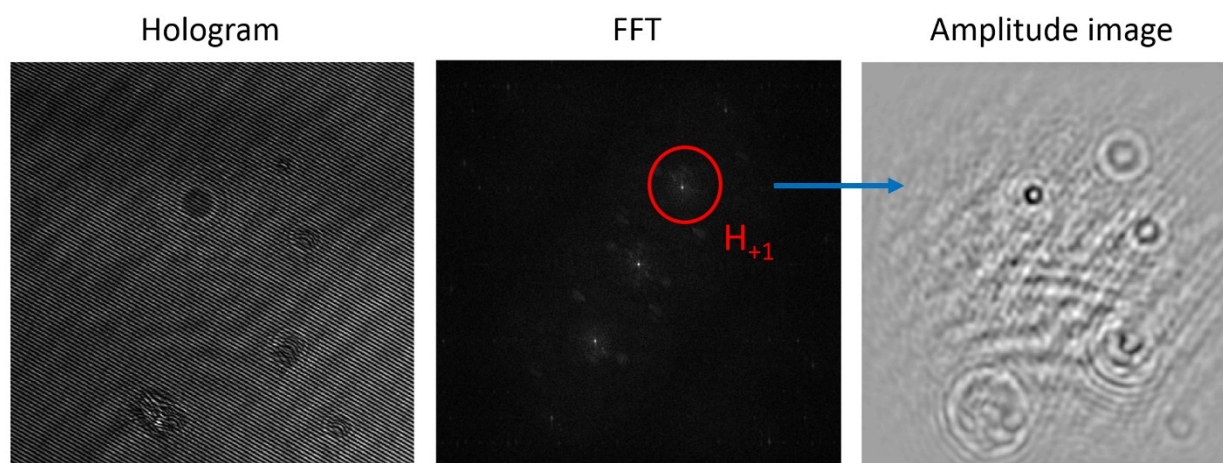
Digital holography (DH) is a technique based on the acquisition of the interference between an object wave (passing through the sample) and a reference wave. Object and reference waves are emitted by the same coherent source and are allowed to interfere. The interference image, known as hologram, is recorded on a digital camera and its intensity distribution in the recording plane is given by:

$$h = |O|^2 + |R|^2 + OR^* + O^*R = H_0 + H_{+1} + H_{-1}, \quad (1)$$

where  $O(x,y,z)$  and  $R(x,y,z)$  are the complex object and reference waves. The dependence on the spatial coordinates is omitted for the sake of brevity. The intensities of the object and reference waves are grouped in  $H_0$ , which is known as the autocorrelation term. The last two are the interference terms; they contain the real and twin images of the complex object. The former is the image that needs to be retrieved.

This problem can be easily solved when using an interferometric setup for off-axis DH, as the one described in Fig. 1 in main text.

In off-axis DH schemes, the reference and object waves meet at the camera sensor forming an angle  $\theta$ , which has the effect of introducing on the hologram a spatial carrier modulated by the object complex term. Hence, the three terms in eq. 2 (i.e.  $H_0$ ,  $H_{+1}$  and  $H_{-1}$ ) are spatially separated in the Fourier domain (Supplementary Fig. S1) and the desired term can be trivially isolated by spatial filtering and demodulation.



Supplementary Fig. S 1. Initial hologram (left), corresponding Fourier spectrum (centre) and reconstructed amplitude image after Fourier filtering and demodulation (right).

It should be noted that, since we employ a digital recording system,  $\theta$  should be properly chosen in order to fulfil the Nyquist requirements<sup>1</sup> for the correct sampling of the interference pattern:

$$\theta_{\max} = \frac{\lambda}{2\Delta p}, \quad (2)$$

where  $\theta_{\max}$  is the maximum value of the angle between reference and object wave,  $\lambda$  is the wavelength of the illumination light and  $\Delta p$  is the pixel size of the digital camera.

Moreover, the off-axis angle has to exceed a minimum value for a proper separation of the diffraction orders.

One should also notice that the size of the diffraction orders influences the capability of isolating them from the autocorrelation term. It has been demonstrated that the size of the orders is connected to the spherical phase distortion introduced by the microscope objective (MO).

In our case, we solve this problem by introducing a MO in each interferometer arm, so that the object and reference wave will have the same curvature in the recording plane. An in-depth analysis of the requirements on the MO features and recording parameters to achieve optimal imaging can be found in Ref. 1.

In our case, we have employed a 20X objective with NA=0.4. The choice of the MO is driven mainly by the need to achieve a compromise between the magnification and the Field of View (FoV).

### **Holographic Tracking Procedure**

Once the interference term containing the real image has been isolated, one can propagate numerically the complex wavefield at different reconstruction planes to recover the object's focus plane. Various algorithms exist for numerical propagation of the hologram, all derived by the solution of the Fresnel-Kirchoff diffraction integral. In our work, we implement the angular spectrum method<sup>2</sup>.

Regardless of the algorithm implemented, this flexible focusing capability is one the most remarkable features of DH, and it is the basis of the implementation of 3D tracking.

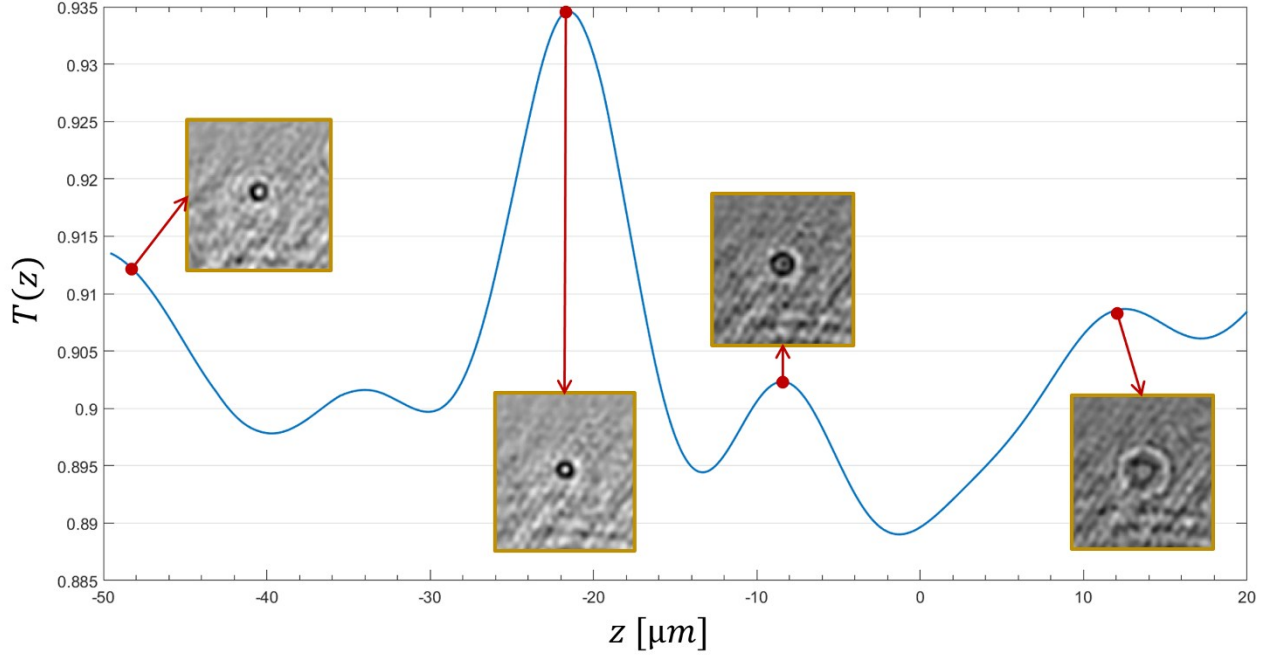
In fact, classical holographic tracking methods are typically articulated in two steps:

- 1) numerical refocusing, to retrieve the position of the object along the optical axis.
- 2) evaluation of the transverse position of focused object.

The first step is thus the axial localization of the object. The optical wavefront is reconstructed at different distances, and for each a suitable image sharpness metric is calculated. Then, a refocusing criterion is applied to identify the focal plane.

Ideally, as in our work we are interested in analysing only the axial displacements of the tracer beads, this step would be sufficient.

However, as it will be showed in the following, the image sharpness metric we chose has made necessary the implementation of a full 3D tracking procedure.



Supplementary Fig. S 2. Calculated Tamura values as a function of the reconstruction distance. The insets show the amplitude images of the propagated object field after propagation at different distances.

A common refocusing criterion is based on the optimization of the Tamura coefficient,  $T = \sqrt{\sigma(I)/\mu(I)}$ , where  $\sigma(\bullet)$  and  $\mu(\bullet)$  are the standard deviation and average operators, respectively and  $I$  is a suitable representation of the image<sup>3</sup>. Depending of the sample,  $I$  can stand for the amplitude (transparent object) or the phase (absorbing object) of the complex field and the refocusing criterion consists respectively in the minimization or maximization of the Tamura coefficient.

In the case of polystyrene beads, we have employed a contrast-based refocusing criterion recently proposed<sup>4</sup>, where  $I = G_d$  is the complex gradient of the propagated image. This representation is especially suited for neither fully transparent nor absorbing objects, as it considers both the amplitude signature and the phase information content. Thus, for any reconstruction distance, we evaluate the Tamura coefficient  $T_d$ , defined as:

$$T_d = \sqrt{\frac{\sigma(G_d)}{\mu(G_d)}} \quad (3)$$

Independently on the absorption properties of the object, the complex gradient image shows sharp boundaries in correspondence of the best focus position. Thus, the focal distance is the one that maximizes  $T_d$ :

$$d_{foc} = \arg \max \{T_d\} \quad (4)$$

Supplementary Fig. S2 shows the behaviour of the Tamura coefficient calculated at different reconstruction distances, and some exemplary reconstructed amplitude images. However, for this criterion it is necessary to select a small region of interest (ROI) around the object. Thus, even for very minute movements of the object in the x-y plane, it is necessary to change the ROI accordingly.

When needed, we have introduced a procedure of transverse localization of the object. In particular, we have employed a centroid-based 2D tracking strategy, applied on in-focus amplitude reconstructions<sup>5</sup>.

#### References:

1. Sánchez-Ortiga, E., Doblaz, A., Saavedra, G., Martínez-Corral, M. & Garcia-Sucerquia, J. Off-axis digital holographic microscopy: practical design parameters for operating at diffraction limit. *Appl. Opt.* **53**, 2058–2066 (2014).
2. Goodman, J. W. *Introduction to Fourier optics*. (McGraw-Hill, 1996).
3. Memmolo, P., Paturzo, M., Javidi, B., Netti, P. A. & Ferraro, P. Refocusing criterion via sparsity measurements in digital holography. *Opt. Lett.* **39**, 4719 (2014).
4. Zhang, Y., Wang, H., Wu, Y., Tamamitsu, M. & Ozcan, A. Edge sparsity criterion for robust holographic autofocusing. *Opt. Lett.* **42**, 3824 (2017).
5. Memmolo, P., Finizio, A., Paturzo, M., Miccio, L. & Ferraro, P. Twin-beams digital holography for 3D tracking and quantitative phase-contrast microscopy in microfluidics. *Opt. Express* **19**, 25833 (2011).